Karlsruhe Institute of Technology

Institute of Electrical Engineering (ETI)
Electrical Drives and Power Electronics
Prof. Dr.-Ing. Michael Braun
Kaiserstr.12. 76131 Karlsruhe

Elektrotechnisches Institut

Title:	FPGA-based real-time simulation of nonlinear permanent magnet synchronous machines for power hardware-in-the-loop emulation systems
Authors:	Schmitt, A.; Richter, J.; Jurkewitz, U.; Braun, M.
Institute:	Elektrotechnisches. Institute. (ETI) - Electrical Drives & Power Electronics, Karlsruhe Institute of Technology (KIT), Karlsruhe, Germany
Type:	Conference Proceedings
Published at:	Industrial Electronics Society, IECON 2014 - 40th Annual Conference of the IEEE; Oct. 29 2014-Nov. 1 2014; Dallas, TX
Hyperlink:	

FPGA-Based Real-Time Simulation of Nonlinear Permanent Magnet Synchronous Machines for Power Hardware-in-the-Loop Emulation Systems

Alexander Schmitt, Jan Richter, Uli Jurkewitz and Michael Braun
Karlsruhe Institute of Technology (KIT)
Elektrotechnisches Institut (ETI) - Electrical Drives and Power Electronics
Kaiserstr. 12, 76131 Karlsruhe, Germany
Phone: +49 721 608-46847
A.Schmitt@kit.edu, www.eti.kit.edu

***Abstract*—This paper presents an FPGA-based real-time simulation system of a nonlinear permanent magnet synchronous machine and its qualification for power hardware-in-the-loop emulation systems. The machine model considers the magnetic anisotropy of the rotor, the saturation of the iron as well as dynamic cross-coupling effects between the direct- and quadrature axis of the machine. A specifically designed high performance signal processing system is developed to calculate the machine behavior with a frequency of 1.5 MHz. The developed model calculates the state variables of the machine as well as the counter voltage for an emulation converter in a way that the coupling network of the power hardware-in-the-loop emulation test bench could be equipped with any inductance. Measurements validate the proper function of the machine model and demonstrate the accurate solution of the nonlinear differential equation system of an anisotropic synchronous machine with nonlinear magnetics in real-time.**

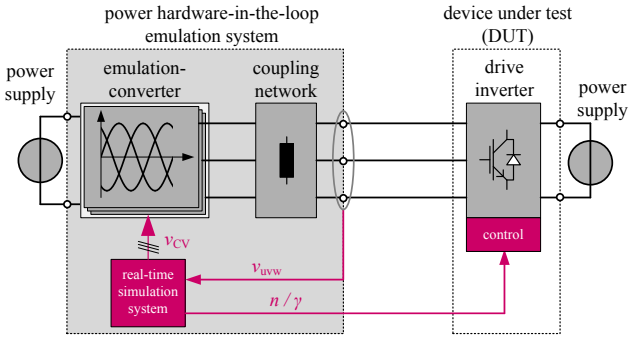

Fig. 1. Schematic diagram of a typical power hardware-in-the-loop emulation test bench.

I. Introduction

In modern drive inverter development processes the importance of simulation increases rapidly [1]. Dependent on the state of development different simulation levels are required to emulate the operating environment of the system [2]. In early stage, various state of the art simulation tools are used to simulate and validate the accurate function of inverters in their operating environments (software-in-the-loop - SIL - simulation). Afterwards, real-time hardware-in-the-loop (HIL) test benches are often used to emulate machines or 3AC-mains to test the developed software in conjunction with the signal processing unit of the power converter. These HIL test benches are well understood and described in literature [3]–[6]. Finally, the converter is commonly connected to a motor-load test bench to improve the performance, reliability or the manufacturing process of the device.

Unfortunately, there are several drawbacks and disadvantages inherent to conventional motorload testbeds. Due to the fact that there are numerous different applications that drives can be used for, various motor-load combinations are required to test the drive inverter. Thus, the space required for the test beds can be exceedingly large and additional costs and maintenance effort are caused [7]. Therefore, it is desirable to connect the converter to be tested to a power hardware-in-the-loop (PHIL) emulation test bench to evaluate its proper function. Figure 1 shows a typical PHIL emulation test bench which is capable to emulate arbitrary electric machines. At this type of test bench, the HIL signal processing unit is extended by an emulation converter which is connected to the device under test (DUT) by means of a coupling network. Dependent on the emulation concept, the coupling network consists of simple chokes or an LCL-Filter-Network [8]. Since the DUT commonly controls the machine currents, the PHIL-emulation system should control the counter voltage at the coupling network which corresponds to the electro-magnetic-force (EMF) to avoid problems caused by a second current controller within the PHIL [9]. Therefore, the EMF of the emulated machine has to be calculated by the HIL system and provided for the emulation converter as reference value. Furthermore, modern permanent magnet synchronous machines (PMSM) often have a magnetic anisotropy and are highly utilized yielding nonlinear magnetics. Hence, saturation and dynamic cross-coupling effects have to be considered in the machine model to ensure an accurate PHIL test bench. In addition, the drive inverter commonly acts as a voltage source. Therefore, the whole machine behavior should be calculated exclusively using the output voltages of the DUT and the load torque as

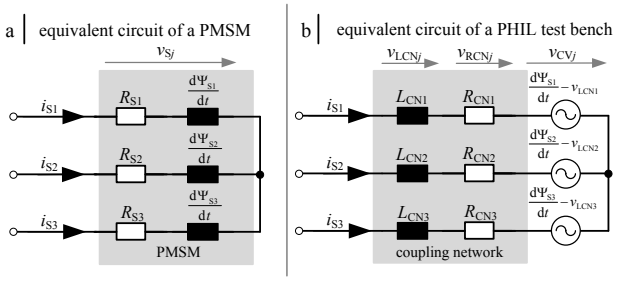

Fig. 2. Equivalent circuit of the PMSM within a PHIL-emulation test bench.

input values. A machine model taking all these effects into account is required which calculates the EMF depending on the stator voltages and adjusts the set value of the counter voltage v_{CV} for the emulation converter in a way that the current slopes through the linear inductors of the coupling network are identical to the current slopes of the real machine. A PMSM model fulfilling these requirements is introduced in Section II. The hardware setup of the specifically designed high performance signal processing system, containing the machine model, is described in Section III. Details about the hardware implementation are reported in Section IV. It has to be considered that the signal processing unit is designed to be used in a PHIL test bench later. Indeed, up to now all measurements were made to validate only the derived machine model and the proper function of the signal processing unit. Therefore, all measurements at the signal processing unit are made with low-level signals and without power flow. The results of these measurements are discussed in Section V. Conclusions are stated in Section VI.

II. Machine Model

In this Section, a computation instruction for the counter voltage $v_{\mathrm{CV}j}$ (Fig. 2b) of an emulation converter is derived in a way that the coupling network of a PHIL test bench could be equipped with any inductance. The basic conditions are that the inductors $L_{\mathrm{CN}j}$ as well as the ohmic resistors $R_{\mathrm{CN}j}$ of the coupling network are linear and identical. Additionally, it is supposed that the resistors of the coupling network $R_{\mathrm{CN}j}$ are identical to the ohmic resistance R_{S} of one phase of the emulated machine. Figure 2a depicts the underlying equivalent circuit of the PMSM. With $j \in \{1,2,3\}$ as phase numbers, the voltage equation of a single PMSM phase is:

$$v_{\mathrm{S}j} = R_{\mathrm{S}j} \cdot i_{\mathrm{S}j} + \frac{\mathrm{d}\,\Psi_{\mathrm{S}j}}{\mathrm{d}t} \tag{1}$$

in which the stator flux linkage $\Psi_{\mathrm{S}j} = \Psi_{\mathrm{S}j}(i_{\mathrm{S1}}, i_{\mathrm{S2}}, i_{\mathrm{S3}}, \gamma)$ depends on the three stator currents $i_{\mathrm{S1}}, i_{\mathrm{S2}}, i_{\mathrm{S3}}$ and the electric rotor position angle γ. However, within a PHIL test bench the coupling network (Fig. 2b) has to be considered in the PMSM machine model. Therefore, the phase equations of the PMSM must be extended by the voltage drop at the coupling inductors $v_{\mathrm{LCN}j}$.

The basic idea of this model is to subtract this voltage drop from the derivation of the flux linkage $\Psi_{\mathrm{S}j}$ to ensure an identical behavior (identical current slopes) of the emulation test bench in comparison to the real machine. This leads to:

$$v_{\mathrm{S}j} = \underbrace{\underbrace{R_{\mathrm{S}j} \cdot i_{\mathrm{S}j}}_{v_{\mathrm{RCN}j}} + \underbrace{L_{\mathrm{CN}j} \cdot \frac{\mathrm{d}i_{\mathrm{S}j}}{\mathrm{d}t}}_{v_{\mathrm{LCN}j}}}_{v_{\mathrm{CN}j}} + \underbrace{\left(\frac{\mathrm{d}\,\Psi_{\mathrm{S}j}}{\mathrm{d}t} - \underbrace{L_{\mathrm{CN}j} \cdot \frac{\mathrm{d}i_{\mathrm{S}j}}{\mathrm{d}t}}_{v_{\mathrm{LCN}j}} \right)}_{v_{\mathrm{CV}j}} \tag{2}$$

in which the term $v_{\mathrm{CV}j}$ is the reference value for the emulation converter of a PHIL test bench. Subsequently, the phase elements $i_{\mathrm{S}j}$, $v_{\mathrm{S}j}$ and $\Psi_{\mathrm{S}j}$ are transformed to the direct (d) and quadrature (q) reference frame with $\underline{z} \in \{\Psi_{\mathrm{S}}, v_{\mathrm{S}}, i_{\mathrm{S}}\}$ and $\underline{a} = e^{\mathrm{j}\frac{2\pi}{3}}$ by:

$$\underline{z} = \frac{2}{3} \cdot \left(x_1 + \underline{a} \cdot x_2 + \underline{a}^2 \cdot x_3\right) \cdot e^{-\mathrm{j}\gamma} \tag{3}$$

With $\Psi_{\mathrm{d,q}} = \Psi_{\mathrm{d,q}}(i_{\mathrm{d}}, i_{\mathrm{q}})$, the machine voltages v_{d} and v_{q} in the dq-reference frame are:

$$\begin{aligned} v_{\mathrm{d}} = & \underbrace{R_{\mathrm{S}} \cdot i_{\mathrm{d}} + L_{\mathrm{CN}} \cdot \frac{\mathrm{d}i_{\mathrm{d}}}{\mathrm{d}t} - \omega L_{\mathrm{CN}} \cdot i_{\mathrm{q}}}_{v_{\mathrm{CN,d}}} \\ & + \underbrace{\frac{\mathrm{d}\,\Psi_{\mathrm{d}}}{\mathrm{d}t} - \omega\,\Psi_{\mathrm{q}} - L_{\mathrm{CN}} \cdot \frac{\mathrm{d}i_{\mathrm{d}}}{\mathrm{d}t} + \omega L_{\mathrm{CN}} \cdot i_{\mathrm{q}}}_{v_{\mathrm{CV,d}}} \end{aligned} \tag{4}$$

and

$$\begin{aligned} v_{\mathrm{q}} = & \underbrace{R_{\mathrm{S}} \cdot i_{\mathrm{q}} + L_{\mathrm{CN}} \cdot \frac{\mathrm{d}i_{\mathrm{q}}}{\mathrm{d}t} + \omega L_{\mathrm{CN}} \cdot i_{\mathrm{d}}}_{v_{\mathrm{CN,q}}} \\ & + \underbrace{\frac{\mathrm{d}\,\Psi_{\mathrm{q}}}{\mathrm{d}t} + \omega\,\Psi_{\mathrm{d}} - L_{\mathrm{CN}} \cdot \frac{\mathrm{d}i_{\mathrm{q}}}{\mathrm{d}t} - \omega L_{\mathrm{CN}} \cdot i_{\mathrm{d}}}_{v_{\mathrm{CV,q}}}. \end{aligned} \tag{5}$$

Both equations are directly sorted in two different parts. Thereby, the first part of the equations is the voltage $v_{\mathrm{CN},x}$ $x \in \{d, q\}$ which considers the voltage drop at the coupling network. The second part corresponds to the counter voltage $v_{\mathrm{CV},x}$ of the coupling network which is the set value for the PHIL emulation converter. Subsequently, according to [10], the derivation of the flux linkages can be resolved to:

$$\frac{\mathrm{d}\,\Psi_{\mathrm{d}}}{\mathrm{d}t} = L_{\mathrm{dd}} \cdot \frac{\mathrm{d}i_{\mathrm{d}}}{\mathrm{d}t} + L_{\mathrm{dq}} \cdot \frac{\mathrm{d}i_{\mathrm{q}}}{\mathrm{d}t} \tag{6}$$

$$\frac{\mathrm{d}\,\Psi_{\mathrm{q}}}{\mathrm{d}t} = L_{\mathrm{qq}} \cdot \frac{\mathrm{d}i_{\mathrm{q}}}{\mathrm{d}t} + L_{\mathrm{qd}} \cdot \frac{\mathrm{d}i_{\mathrm{d}}}{\mathrm{d}t}. \tag{7}$$

Thereby, dynamic cross-coupling and saturation effects are considered. It has to be kept in mind, that L_{dd}, L_{qq}, L_{dq} and L_{qd} are differential inductances and therefore functions of i_{d} and i_{q} in this representation. Substitution of (6) and (7)

in (4) and (5) and solving for the current derivatives yields:

$$\frac{\mathrm{d}i_\mathrm{d}}{\mathrm{d}t} = \frac{v_\mathrm{d} - R_\mathrm{S}\cdot i_\mathrm{d} + \frac{L_\mathrm{dq}}{L_\mathrm{qq}}\left(-v_\mathrm{q} + R_\mathrm{S}\cdot i_\mathrm{q} + \omega\,\Psi_\mathrm{d}\right) + \omega\,\Psi_\mathrm{q}}{L_\mathrm{dd} - \frac{L_\mathrm{dq}\cdot L_\mathrm{qd}}{L_\mathrm{qq}}} \tag{8}$$

$$\frac{\mathrm{d}i_\mathrm{q}}{\mathrm{d}t} = \frac{v_\mathrm{q} - R_\mathrm{S}\cdot i_\mathrm{q} + \frac{L_\mathrm{qd}}{L_\mathrm{dd}}\left(-v_\mathrm{d} + R_\mathrm{S}\cdot i_\mathrm{d} - \omega\,\Psi_\mathrm{q}\right) - \omega\,\Psi_\mathrm{d}}{L_\mathrm{qq} - \frac{L_\mathrm{dq}\cdot L_\mathrm{qd}}{L_\mathrm{dd}}}. \tag{9}$$

Finally, the counter voltage $v_{\mathrm{CN},x}$, considering the voltage drop at the coupling inductors as well as the saturation and the anisotropy of the machine can be calculated to:

$$\begin{aligned} v_\mathrm{CV,d} &= i_\mathrm{q}\cdot\omega\cdot L_\mathrm{CN} + \frac{\mathrm{d}i_\mathrm{d}}{\mathrm{d}t}\left(L_\mathrm{dd} - L_\mathrm{CN}\right) \\ &\quad + \frac{\mathrm{d}i_\mathrm{q}}{\mathrm{d}t}\cdot L_\mathrm{dq} - \Psi_\mathrm{q}\cdot\omega \end{aligned} \tag{10}$$

$$\begin{aligned} v_\mathrm{CV,q} &= -i_\mathrm{d}\cdot\omega\cdot L_\mathrm{CN} + \frac{di_\mathrm{q}}{\mathrm{d}t}\left(L_\mathrm{qq} - L_\mathrm{CN}\right) \\ &\quad + \frac{\mathrm{d}i_\mathrm{d}}{\mathrm{d}t}\cdot L_\mathrm{qd} + \Psi_\mathrm{d}\cdot\omega \end{aligned} \tag{11}$$

and the derivation of the equations for the electric system of the PMSM is completed. The mechanical system of the machine is described with the equation for the inner torque M_i:

$$M_\mathrm{i} = \frac{3}{2}\cdot p\left(\Psi_\mathrm{d}\cdot i_\mathrm{q} - \Psi_\mathrm{q}\cdot i_\mathrm{d}\right) \tag{12}$$

and the equation for the electric rotor speed ω as integration of the accelerating torque:

$$\omega = \frac{p}{J}\int_{t=0}^{T}\left(M_\mathrm{i} - M_\mathrm{L}\right)\mathrm{d}t \tag{13}$$

whereby, J is the inertia torque, M_L equals the load torque and p is the number of pole pairs of the machine. The machine equation shall be solved on an FPGA with a frequency of $f_\mathrm{model} = 1.5\,\mathrm{MHz}$. For this reason, the equations have to be discretized. Due to the fact that the simulation time-step $\Delta T_\mathrm{model} = \frac{1}{f_\mathrm{model}} = 667\,\mathrm{ns}$ is several orders of magnitude smaller in comparison to the electric time constant of the machine, the equations (8) to (13) can be discretized using the Forward Euler method without losing significant accuracy or stability [11]. The discretized equation to calculate the d-current in the next time step $t = t(k+1)$ with $k \in \mathbb{N}$ is:

$$i_\mathrm{d,k+1} = i_\mathrm{d,k} + \Delta i_\mathrm{d} \tag{14}$$

with (8)

$$\begin{aligned} \Delta i_\mathrm{d} &= \Delta T_\mathrm{model}\cdot\frac{v_\mathrm{d,k} - R_\mathrm{S}\cdot i_\mathrm{d,k} + \omega_\mathrm{k}\,\Psi_\mathrm{q,k}}{K_\mathrm{d}} \\ &\quad + \frac{\frac{L_\mathrm{dq}}{L_\mathrm{qq}}\left(-v_\mathrm{q,k} + R_\mathrm{S}\cdot i_\mathrm{q,k} + \omega_\mathrm{k}\,\Psi_\mathrm{d,k}\right)}{K_\mathrm{d}} \end{aligned} \tag{15}$$

and

$$K_\mathrm{d} = L_\mathrm{dd} - \frac{L_\mathrm{dq}\cdot L_\mathrm{qd}}{L_\mathrm{qq}}. \tag{16}$$

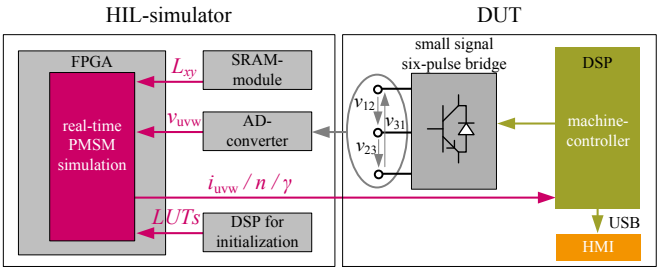

Fig. 3. Schematic diagram of the current HIL test bench.

The discretization in the q-axis leads to:

$$i_\mathrm{q,k+1} = i_\mathrm{q,k} + \Delta i_\mathrm{q} \tag{17}$$

with (9)

$$\begin{aligned} \Delta i_\mathrm{q} &= \Delta T_\mathrm{model}\cdot\frac{v_\mathrm{q,k} - R_\mathrm{S}\cdot i_\mathrm{q,k} - \omega_\mathrm{k}\,\Psi_\mathrm{q,k}}{K_\mathrm{q}} \\ &\quad + \frac{\frac{L_\mathrm{qd}}{L_\mathrm{dd}}\left(-v_\mathrm{d,k} + R_\mathrm{S}\cdot i_\mathrm{d,k} - \omega_\mathrm{k}\,\Psi_\mathrm{d,k}\right)}{K_\mathrm{q}} \end{aligned} \tag{18}$$

and

$$K_\mathrm{q} = L_\mathrm{qq} - \frac{L_\mathrm{dq}\cdot L_\mathrm{qd}}{L_\mathrm{dd}}. \tag{19}$$

The calculation instruction for the counter voltage is discretized:

$$\begin{aligned} v_\mathrm{CV,d,k+1} &= i_\mathrm{q,k}\cdot\omega_\mathrm{k}\cdot L_\mathrm{CN} + \Delta i_\mathrm{d}\left(L_\mathrm{dd} - L_\mathrm{CN}\right) \\ &\quad + \Delta i_\mathrm{q}\cdot L_\mathrm{dq} - \Psi_\mathrm{q,k}\cdot\omega_\mathrm{k} \end{aligned} \tag{20}$$

and

$$\begin{aligned} v_\mathrm{CV,q,k+1} &= -i_\mathrm{d,k}\cdot\omega_\mathrm{k}\cdot L_\mathrm{CN} + \Delta i_\mathrm{q}\left(L_\mathrm{qq} - L_\mathrm{CN}\right) \\ &\quad + \Delta i_\mathrm{d}\cdot L_\mathrm{qd} + \Psi_\mathrm{d,k}\cdot\omega_\mathrm{k}. \end{aligned} \tag{21}$$

The inner torque of the machine is discretized calculated to:

$$M_\mathrm{i,k+1} = \frac{3}{2}\cdot p\left(\Psi_\mathrm{d,k}\cdot i_\mathrm{q,k} - \Psi_\mathrm{q,k}\cdot i_\mathrm{d,k}\right) \tag{22}$$

and the rotational speed is:

$$\omega_\mathrm{k+1} = \omega_\mathrm{k} + \Delta T_\mathrm{model}\cdot\frac{p}{J}\left(M_\mathrm{i,k} - M_\mathrm{L,k}\right) \tag{23}$$

After back transformation of these equations to the coordinate system fixed to the stator, a time-discrete computation instruction for an unbalanced nonlinear PMSM is derived. This instruction can be calculated by the signal processing unit of a PHIL-emulation system.

III. Hardware Setup

In this Section the specifically designed high performance signal processing unit is introduced, which calculates the derived equations from Section II. A HIL test bench is build up to validate the machine equations. A schematic diagram of the build up HIL test bench is shown in Fig. 3. The hardware setup is designed to be as similar as possible to the real-time simulation system which is needed for a PHIL test bench to ensure an easy integration of the signal processing unit

TABLE I
MACHINE PARAMETERS

Parameter	Value
Voltage nom.	212 V
Current nom. / max.	169 A / 300 A
Shaft power nom. / max.	57 kW / 97 kW
Speed nom. / max.	4200 min^{-1} / 11000 min^{-1}
Torque nom. / max.	130 Nm / 220 Nm
Inertia torque	0.06 $\mathrm{kg} \cdot \mathrm{m}^2$
Ohmic stator resistance typ.	10.5 mΩ
Number of pole pairs	3
Ohmic resistance of the supposed coupling network typ.	10.5 mΩ
Inductance of the supposed coupling network typ.	1.2 mH

in a PHIL test bench subsequently. The interface between a PHIL test bench and the DUT are the output voltages of the DUT. Therefore, the FPGA is directly connected to THS 1206 A/D-converters from Texas Instruments with a sample rate of 1.5 MHz to measure the pulsed output voltages of the DUT as input values for the machine model.

A. HIL Simulator

The core of the HIL simulator is an FPGA-board with a Cyclone 4 FPGA (EP4CE40F23C6) from Altera. This device contains 39600 logic cells and 116 embedded 18 x 18 multipliers. The FPGA-board has double euroboard format and is built as plug-in unit for a 19" rack. Since the values of the flux linkages Ψ_x and the inductances L_{xy} $x, y \in \{d, q\}$ are depending on the instantaneous machine currents $i_{\mathrm{d,k}}$ and $i_{\mathrm{q,k}}$, look-up tables (LUT) of these values are stored in two external 4 MB SRAM modules which are connected to the FPGA. The reciprocals of the numerators K_{d} (16) and K_{q} (19) in equation (15) and (18) are also stored in a LUT to avoid two divisions. Due to the fact that SRAM is a volatile storage, the LUTs of the machine model are transferred by means of a digital signal processor to the FPGA and from there to the SRAM at the beginning of the simulation. The LUT grid has a resolution of 2 A and the values are stored with an accuracy of 16 Bit. All model parameters such as flux linkages, differential inductances or the ohmic stator resistance are obtained by machine measurements. A motor manufactured by Brusa of type HSM1-6.1712-C01 is used for that purpose [12]. This machine is an interior permanent magnet synchronous machine (IPMSM) with a strong reluctance torque. Figure 4 illustrate the measured d- and q-flux linkages. Both characteristics are nonlinear due to saturation and cross-coupling. Saturation causes the s-shaped trend of the flux linkage Ψ_{d} in case that i_{d} is changed as well as in the flux linkage Ψ_{q} if i_{q} is changed. Cross-coupling in contrary leads to the distortion of Ψ_{d} if i_{q} is modified and of Ψ_{q} if i_{d} is modified. The basic parameters of the machine as well as the parameters of the supposed coupling network are shown in Table I.

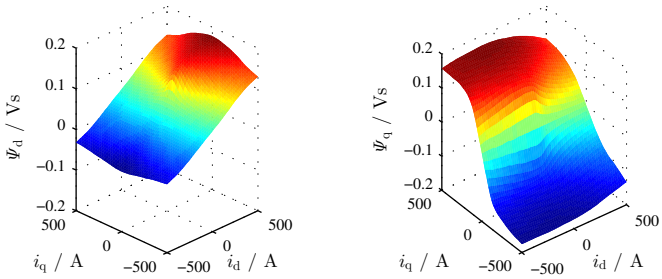

Fig. 4. Flux linkage Ψ_{d} (left) and flux linkage Ψ_{q} (right)

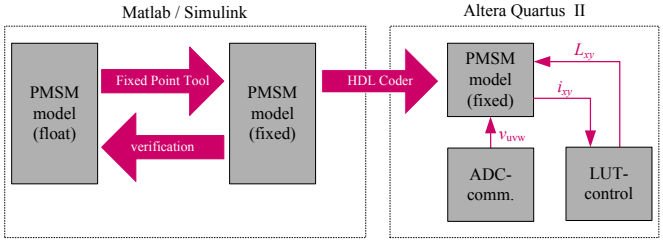

Fig. 5. Workflow of the PMSM model verification as well as the VHDL-code generation.

B. Device Under Test

The core of the DUT (Fig. 3) is a DSP from Texas Instruments (TMS320C6748) which executes the machine controller with a control frequency of $f_{\mathrm{c}} = 8$ kHz. The HIL simulator is controlled by a nonlinear current controller for saturated cross-coupled PMSMs described in [13]. Since the current hardware setup is only designed for low-level signals, the machine controller pulses a small signal six-pulse bridge, realized with bipolar transistors, to generate the required pulsed output voltage for the A/D-converter of the signal processing unit. It has to be considered that the switching characteristic of a bipolar transistor is different from the switching characteristic of an IGBT, though this difference could be neglected because only the machine model should be validated initially. The human-machine interface (HMI) which controls the DUT is a standard personal computer (PC) with a graphical user interface implemented in LabVIEW. The PC is connected to the DSP via USB. It has to be noted that the values of the machine currents, rotor angle and speed are directly transferred from the FPGA to the DSP of the DUT.

IV. Hardware Implementation

The implementation of the machine model is performed using the Matlab Fixed-Point Tool, and the Matlab HDL Coder to ensure a HIL respectively PHIL test bench with maximum flexibility (Fig. 5). Therefore, the machine model is first implemented and verified in Simulink using floating point representation. Subsequently, the model is converted to a custom fixed point format by means of the Matlab Fixed-Point Tool. The results of the fixed point implementation are compared with the float model to check the accuracy. The model was generated with an accuracy of 20 Bit decimal places and a variable word length according to the maximum

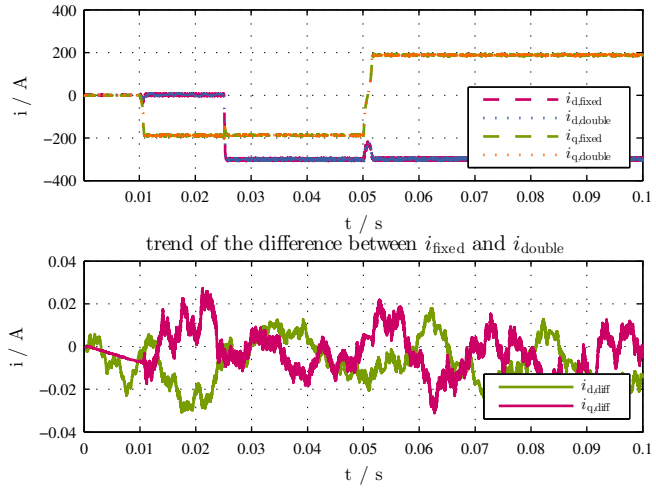

Fig. 6. Comparison of the accuracy between the fixed and the floating point representation of the PMSM model.

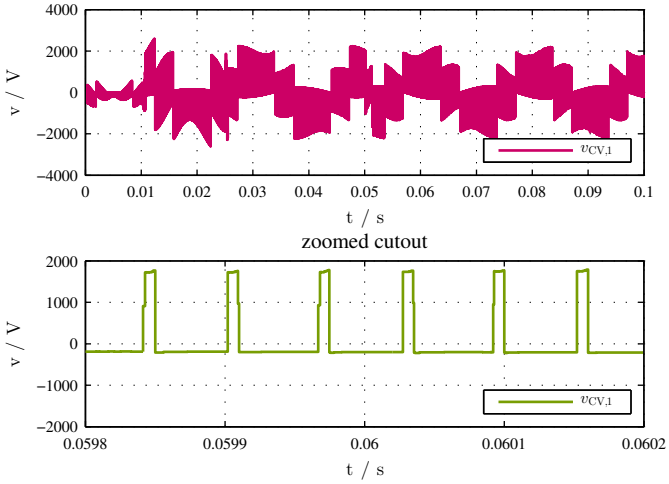

Fig. 7. Waveform of the calculated counter voltage for the emulation converter of a PHIL test bench.

value of the state variables. The sine and cosine of the rotor angle γ for the vector transformation is calculated with the CORDIC-algorithm directly in the FPGA.

A. Accuracy of the Model

The model was set to a constant rotational speed of $500\,\mathrm{min}^{-1}$ to verify the accuracy of the fixed point representation. Thereafter, the current controller impresses a d-current of $-300\,\mathrm{A}$ and a q-current of $\pm 185\,\mathrm{A}$. The simulation was executed in Matlab / Simulink. The waveforms of the model currents i_d and i_q are shown in Fig. 6 (first plot). The second plot shows the difference between the currents from the floating point- and the fixed point model. It can be seen that the difference of the currents are in the dimension of tens of milli ampere. Hence, the relative error is less than 0.01% and therefore, the difference can be neglected and the fixed point implementation is adequate.

B. Simulation of the EMF

Due to the minor sampling time of the DSP compared with the FPGA it is not possible to read all calculated values for the EMF out of the FPGA. Hence, the waveform of the counter voltage for the coupling network is only validated using the simulation in Matlab / Simulink. The boundary conditions are the same as for the accuracy test. The trend of the counter voltage is plotted for one phase in Fig. 7. It has to be considered that the counter voltage waveform has spikes up to 3000 V. These spikes are necessary because the PHIL test bench should ensure the correct current slopes in the coupling inductors of the emulation system during the active as well as the freewheeling switching states of the DUT. Indeed, in the final PHIL test bench it is not possible to generate an output voltage with this waveform because of the limited DC link voltage as well as the limited modulation frequency of the emulation converter. Though, the integration of the calculated counter voltage over the time will solve this problem, if the required voltage time area will be set as short time mean value with an explicit higher frequency than the switching frequency of the DUT. A modular multiphase multilevel converter (MMPMC) as proposed in [14] seems to be suitable for this application.

V. Measurements

Finally, the fixed point model was translated to the hardware description language VHDL by means of the Matlab / Simulink HDL Coder and embedded in the custom FPGA-design including the communication with the A/D-converter and the SRAM for the LUTs. Subsequently, measurements at the HIL test bench as well as on a real motor test bench were performed to evaluate the proper function of the implemented machine model on the signal processing unit.

A. HIL Test Bench

The measurements at the HIL test bench were also performed with a constant rotational speed of ($500\,\mathrm{min}^{-1}$). At the beginning, the set value i_ref of the d-current controller is $-300\,\mathrm{A}$ and the set value of the q-current is $-185\,\mathrm{A}$. This current combination equates a random point at the maximum torque per ampere (MTPA) line of the PMSM. At $t = 0\,\mathrm{s}$ the desired value of the q-current controller is set to $185\,\mathrm{A}$. Figure 8 shows the waveform of the currents calculated on the FPGA. It has to be considered that the values are read out of the FPGA by means of the DUT every $125\,\mu\mathrm{s}$. Therefore, the plot does not contain data points for all calculated time steps. However, in the zoomed cutout, it can be recognized that the current change is nonlinear during the single sampling intervals which is caused by saturation of the machine. In order to demonstrate the accuracy of the underlying machine model, the dynamic decoupling feature of the used current controller is disabled. Thus, the d-current changes due to dynamic cross-coupling during the q-current step.

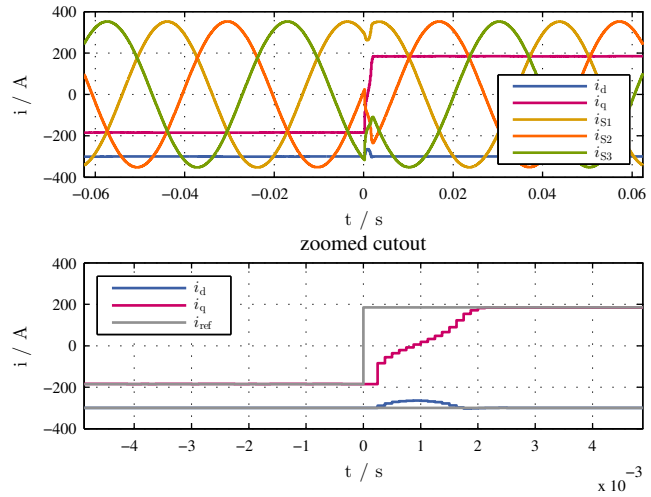

Fig. 8. Trend of the calculated real-time PMSM model current waveforms during a step of the desired q-current at the HIL test bench.

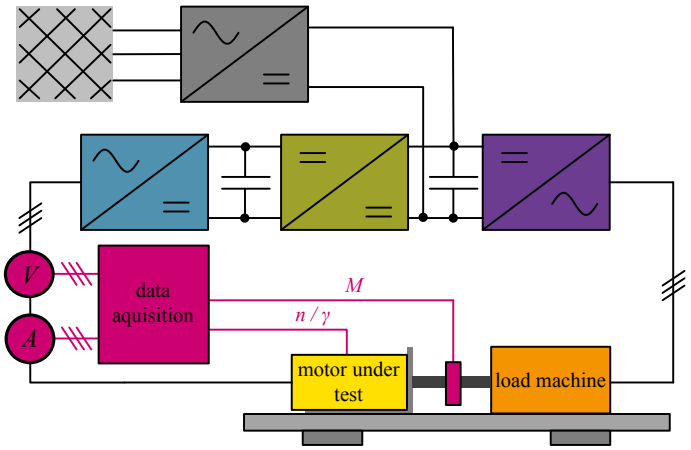

Fig. 9. Schematic diagram of the motor test bench.

B. Motor Test Bench

Finally, the validation of the model was completed by a comparison between the results of the calculated PMSM model on the HIL test bench and measurements at the real motor. Figure 9 shows the schematic diagram of the used motor test bench. The test bench is connected to the grid by means of an active front end converter (grey) that feds the main DC link. The converter which controls the load machine (purple) is also connected to this DC link. An other converter (blue) is used to control the motor under test. This converter is connected to the main DC link by means of a DC-DC-converter (green) which provides the opportunity to generate a second independent DC link voltage for the motor under test. The machine described in Section III with the parameters shown in Table I and Fig. 4 is used as motor under test. The load machine is an induction machine by Wittur. During the measurements, the induction machine was speed controlled and ensures the constant rotational speed of $500\,\mathrm{min}^{-1}$ to ensure similar circumstances compared to the HIL test bench.

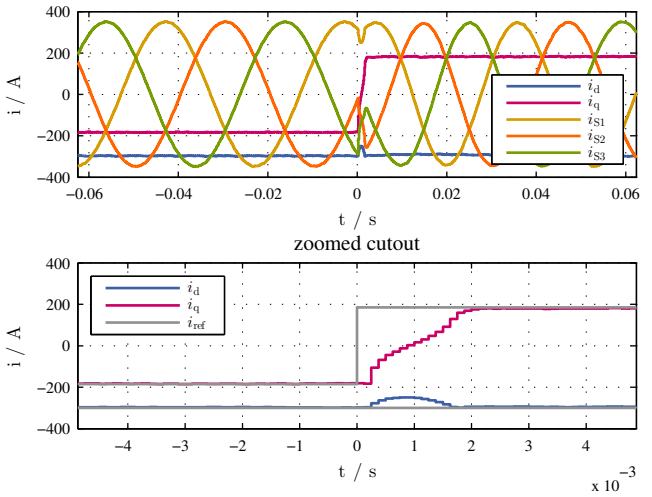

Fig. 10. Trend of the measured PMSM current waveforms during a step of the desired q-current at the motor test bench.

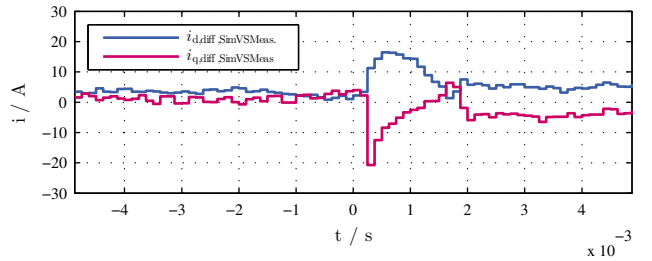

Fig. 11. Difference between the currents in the HIL- and the motor test bench.

Figure 10 depicts the currents which were measured at the PMSM on the motor test bench. The nonlinear increase of the q-current which is caused by saturation as well as the change of the d-current due to dynamic cross-coupling are almost identical to the HIL results given in Fig. 8. In Fig. 11, the difference between the HIL model and the real machine is calculated. The remaining differences are relatively small and caused by the nonlinearity of the machine converter (the demanded voltage time area of the controller is different from the applied voltage time area of the inverter) and the load dependent voltage change of the DC link voltage.

VI. Conclusion

This paper presents an FPGA-based real-time simulation system of a nonlinear PMSM especially for PHIL emulation systems. The machine model considers the magnetic anisotropy of the rotor, the iron saturation as well as dynamic cross-coupling effects between the d- and q-axis of the machine. A specifically designed high performance signal processing system is developed to calculate the machine behavior depending on the measured stator voltage with a frequency of $1.5\,\mathrm{MHz}$. The machine model is implemented in Matlab / Simulink and translated by means of the Matlab Fixed-Point Tool and the HDL Coder in VHDL. The model calculates the counter voltage of the machine as desired value for a PHIL

emulation converter in a way that the coupling network of the PHIL test bench could be equipped with any inductance. Measurements at the HIL test bench as well as on the real machine validate the proper function of the machine model and demonstrate the accurate solution of the nonlinear differential equation system in real-time. Concluding, it is now possible to include the described machine model in a PHIL test bench to achieve a realistic emulation of an anisotropic PMSM with nonlinear magnetics.

REFERENCES

[1] D. Maclay, "Simulation gets into the loop," *IEE Review*, vol. 43, no. 3, pp. 109–112, May 1997.

[2] A. Bouscayrol, "Different types of hardware-in-the-loop simulation for electric drives," in *Industrial Electronics, 2008. ISIE 2008. IEEE International Symposium on*, 2008, pp. 2146–2151.

[3] C. Dufour, S. Cense, T. Yamada, R. Imamura, and J. Belanger, "Fpga permanent magnet synchronous motor floating-point models with variable-dq and spatial harmonic finite-element analysis solvers," in *Power Electronics and Motion Control Conference (EPE/PEMC), 2012 15th International*, 2012, pp. LS6b.2–1–LS6b.2–10.

[4] M. Matar and R. Iravani, "Massively parallel implementation of ac machine models for fpga-based real-time simulation of electromagnetic transients," *Power Delivery, IEEE Transactions on*, vol. 26, no. 2, pp. 830–840, April 2011.

[5] L. Herrera and J. Wang, "Fpga based detailed real-time simulation of power converters and electric machines for ev hil applications," in *Energy Conversion Congress and Exposition (ECCE), 2013 IEEE*, Sept 2013, pp. 1759–1764.

[6] M. Oettmeier and C. Heising, "Fpga-based pmsm emulation: Concept and verification," *PCIM Europe, Nuernberg*, 2012.

[7] S. Grubic, B. Amlang, W. Schumacher, and A. Wenzel, "A high-performance electronic hardware-in-the-loop drive-load simulation using a linear inverter (linverter)," *Industrial Electronics, IEEE Transactions on*, vol. 57, no. 4, pp. 1208–1216, 2010.

[8] S. Lentijo, S. D'Arco, and A. Monti, "Comparing the dynamic performances of power hardware-in-the-loop interfaces," *Industrial Electronics, IEEE Transactions on*, vol. 57, no. 4, pp. 1195–1207, 2010.

[9] R. Kennel, T. Boller, and J. Holtz, "Replacement of electrical (load) drives by a hardware-in-the-loop system," in *Electrical Machines and Power Electronics and 2011 Electromotion Joint Conference (ACEMP), 2011 International Aegean Conference on*, 2011, pp. 17–25.

[10] J. Richter, P. Winzer, and M. Doppelbauer, "Einsatz virtueller Prototypen bei der akausalen Modellierung und Simulation von permanenterregten Synchronmaschinen," in *Internationaler ETG-Kongress 2013 (ETG-FB 139)*, 2013.

[11] L. Wang, J. Jatskevich, and H. Dommel, "Re-examination of synchronous machine modeling techniques for electromagnetic transient simulations," *Power Systems, IEEE Transactions on*, vol. 22, no. 3, pp. 1221–1230, Aug 2007.

[12] J. Richter, A. Dollinger, and M. Doppelbauer, "Iron loss and parameter measurement of permanent magnet syncronous machines," *ICEM, Berlin*, September 2014 (unpublished, accepted).

[13] J. Richter, T. Gemassmer, and M. Doppelbauer, "Predictive current control of saturated cross-coupled permanent magnet synchronous machines," in *International Symposium on Power Electronics, Electrical Drives, Automation and Motion*, June 2014, pp. 823–828.

[14] A. Schmitt, M. Gommeringer, J. Kolb, and M. Braun, "A high current, high frequency modular multiphase multilevel converter for power hardware-in-the-loop emulation," in *PCIM Europe 2014; International Exhibition and Conference for Power Electronics, Intelligent Motion, Renewable Energy and Energy Management; Proceedings of*, May 2014, pp. 1–8.

Alexander Schmitt was born in Bad Mergentheim, Germany in 1984. He received the Dipl.-Ing. degree from the Karlsruhe Institute of Technology (KIT), Karlsruhe, Germany in 2010. Since 2010 he works as a doctoral candidate at the Institute of Electrical Engineering (ETI) which is located at the Karlsruhe Institute of Technology (KIT). His research interests are multilevel converters and power hardware-in-the-loop emulation systems.

Jan Richter was born in Heidelberg, Germany in 1984. He graduated from Karlsruhe Institute of Technology (KIT) with his diploma in 2011. In June 2011 he started to work as a doctoral candidate at the Institute of Electrical Engineering (ETI) at KIT in the field of modelling, parameter identification and control of permanent magnet synchronous machines.

Uli Jurkewitz was born in Heidelberg Germany in 1986. He received his B.Sc. degree from the Karlsruhe Institute of Technology (KIT), Karlsruhe, Germany in 2012. Since 2012 he is a graduand student at the Karlsruhe Institute of Technology. His study model is electrical drives and power electronics which is supported by the Institute of Electrical Engineering (ETI), located at the KIT.

Michael Braun received the Dipl.-Ing. and Dr.-Ing. degrees from the Technische Hochschule Darmstadt, Germany, in 1978 and 1983, respectively. From 1983 to 1994, he was with Siemens AG, Erlangen, Germany, where he was engaged in the development of power electronics and electrical drives. Since 1994, he has been a Professor and the Head of the Institute of Electrical Engineering (ETI), Karlsruhe Institute of Technology, Germany. His research interests include power electronics, control of electrical drives, and mechatronics.